GestureLSM: Latent Shortcut based Co-Speech Gesture Generation with Spatial-Temporal Modeling

Pinxin Liu, Luchuan Song*, Junhua Huang, Chenliang Xu
University of Rochester

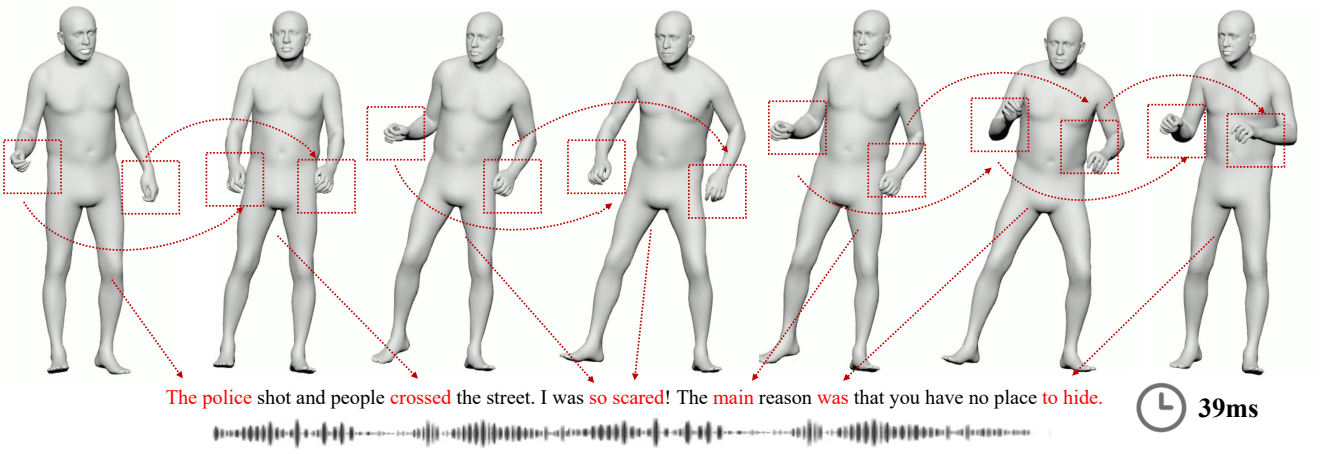

Figure 1. **We present GestureLSM**, a method that explicitly models the body part interactions to achieve smooth overall gesture motions while also capable of real-time generation based on shortcut sampling.

Abstract

Controlling human gestures based on speech signals presents a significant challenge in computer vision. While existing works did preliminary studies of generating holistic co-speech gesture from speech, the spatial interaction of each body region during the speech remains barely explored. This leads to wield body part interactions given the speech signal. Furthermore, the slow generation speed limits the construction of real-world digital avatars. To resolve these problems, we propose ***GestureLSM****, a Latent Shortcut based approach for Co-Speech Gesture Generation with spatial-temporal modeling. We tokenize various body regions and explicitly model their interactions with spatial and temporal attention. To achieve real-time gesture generations, we exam the denoising patterns and design an effective time distribution to speed up sampling while improve the generation quality for shortcut model. Extensive quantitative and qualitative experiments demonstrate the effectiveness of GestureLSM, showcasing its potential for various applications in the development of digital humans and embodied agents. Project Page:* https://andypinxinliu.github.io/GestureLSM

*corresponding author.

1. Introduction

In everyday conversations, speech always comes with gestures that try to convey emotions and enhance understandings [9]. These non-verbal cues play a vital role in effective interaction [3], gesture generation a key component of natural human-computer interactions. As artificial intelligence advances, equipping virtual avatars with realistic gesture capabilities will become essential in creating immersive interactive experiences.

Many recent works [5, 23, 27, 40] have conducted preliminary studies on co-speech gesture generation. These methods typically treat human body motions and facial expressions as a unified motion feature, represented using either continuous [1] or discrete vq tokens [25, 41]. By encoding speech signals to learn gesture triggers, they aim to generate holistic human body motions.

While these approaches have demonstrated plausible gesture patterns for individual body regions, they often produce unnatural global movements. This issue stems from their unified motion feature learning process, which overlooks the nuanced interactions between different body parts.

For instance, when expressing the sentence ”I completely agree,” natural gestures involve intricate coordination: the fingers might point or emphasize, the arms could

extend outward, and the torso might subtly shift to convey affirmation. However, unified motion representations constrain models from learning such fine-grained interactions, leading to uncoordinated and unnatural gesture patterns. These limitations not only hinder the realism of generated gestures but also restrict their applications in industry-grade animations.

Moreover, many existing models employ either diffusion-based approaches [5, 6] or autoregressive generation methods [25, 41]. Diffusion models rely on iterative denoising processes, while autoregressive models decode gestures token by token. Both methods significantly slow down inference, further exacerbating challenges in real-time deployment.

To address these issues, we propose **GestureLSM**: a real-time Latent Shortcut Model for Co-Speech Gesture Generation with spatial-temporal modeling. Our method explicitly models interactions between different body parts by dividing the human body into four components: upper body, hands, lower body, and facial expressions. Using residual vector quantization, we define distinct motion representations for each part. During generation, we apply spatial and temporal attention to enable more natural interactions among body parts, guided by speech triggers. To accelerate the generation process, we adopt a latent shortcut approach, significantly speeding up diffusion sampling. We further explored the denoising patterns and effectively design the time distribution sampling for training that further enhance the generation quality and speed. Both quantitative and qualitative experiments demonstrate that GestureLSM achieves superior generation quality compared to existing methods while significantly improving inference speed. In summary, our primary contributions are:

1. We present *GestureLSM*, a framework that achieves high quality and real-time co-speech gesture generation.
2. We construct *spatial-temporal modeling* that significantly improve gesture generation by building interactions between different body regions.
3. We analyze denoising patterns, and explore an effective time sampling for training to improve shortcut generation.

2. Related Works

Co-speech Gesture Generation Most recent works on co-speech gesture generation employ skeleton- or joint-level pose representations. [14] use an adversarial framework to predict hand and arm poses from audio, and leverage conditional generation [4] based on pix2pixHD [37] for videos. Some recent works [10, 27, 39] learns the hierarchical semantics or leverage contrastive learning to obtain joint audio-gesture embeding to assist the gesture pose generation. HA2G [27] construct high and low level audio-motion embedding for gesture generation. TalkShow [41] estimates SMPL [31] poses, and models the body and hand motions for talk-show videos. CaMN [24] and EMAGE [25] propose a large scale conversational and speech datasets for joint face and body modeling with diverse style control, with GPT-style decoding for gesture generation.

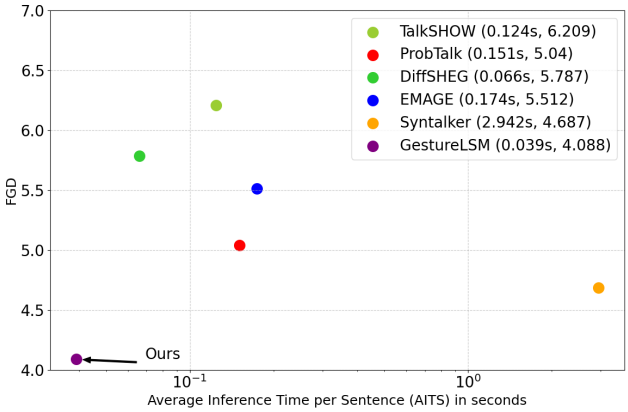

Figure 2. GestureLSM achieves significant generation quality improvement over SOTA methods with fastest inference speed.

MambaTalk [40] speeds up the generation process with efficient mamba structure. Semantic Gesticulator [44] enhances the gesture generation with semantic annotation of gesture types and triggers for retrieval. DiffSHEG [6] and SynTalker [5] build up a diffusion-based gesture generation pipeline. However, none of these works consider the interactions of different body regions conditioned on speech input and achieve fast and real-time gesture generations.

Fast Diffusion Sampling Diffusion models [16] have demonstrated impressive generation quality across various modalities [2, 32], but they suffer from slow inference speeds due to their iterative sampling process. To address these efficiency challenges, several approaches have been proposed, such as Consistency Models [30, 34] and Diffusion Distillations [33, 42]. However, these methods still face limitations in terms of training speed and flexibility.

One promising direction for improving inference speed is the use of flow matching. [26] introduces rectified flow, which provides a crucial baseline for diffusion acceleration. Through rectification, they straighten the ODE path of flow-matching-based diffusion models. Building on this, [28, 36, 45] scales rectified flow to large-scale text-to-image generation, achieving one-step generation.

Shortcut Models [13] further unified the distillation with flow matching. It considers the distance for the future curvature and explicitly allow the model to predict a shortcut along the sampling trajectory through self consistency. Based on this, we further analyze the denoising patterns and explore the time distribution sampling to further enhance the generation quality and inference speed for speech driven gesture generation domain.

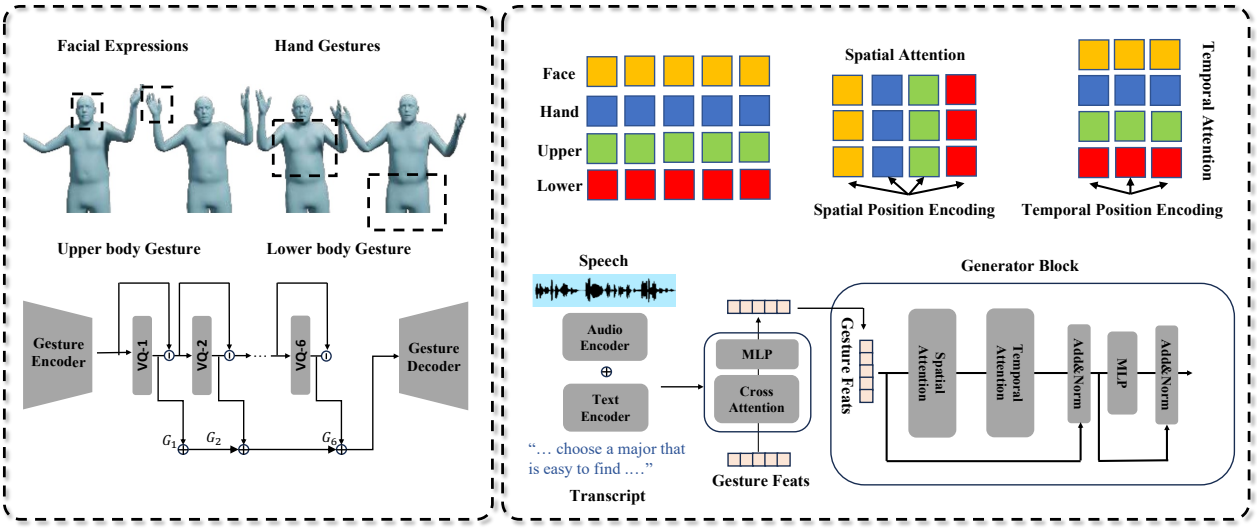

Figure 3. **Left**: Different Body Region Gesture Representation Encoding with Residual Vector Quantization. **Right**: We leverage spatial-temporal attention with position encoding to learn the interaction of body regions given speech input.

3. GestureLSM

As illustrated in Fig.3, our method achieves fast speech driven gesture generation with fine-grained spatial-temporal control. We first construct the gesture motion representation as different body joint groups in Sec. 3.1. To achieve the learning of interactions of different body joints, we leverage spatial-temporal attention in Sec. 3.2. We achieve real-time gesture generations through Rectified Diffusion in Sec. 3.3

3.1. Speech-Gesture Feature Representation

Gesture Body Region Quantization. We construct RVQ quantizers [18] to convert the local body motions, namely hands, upper body, and leg motions, into discrete tokens, as illustrated on the left of Fig. 3.

For each body joint group with sequence length T, we employ a convolutional network to encode the body region $\mathbf{B} = \{\mathbf{b}_t\}_{t=1,\dots,T}$ into vectors $\mathbf{V} = \{\mathbf{v}_t\}_{t=1,\dots,T}$, where each vector $\mathbf{v}_t$ corresponds to time t, by the encoder network $\mathcal{E}$, composed of two convolutional residual blocks. Then we quantize the vector with a codebook $\mathbf{C} = \{\mathbf{c}_i\}_{i=1}^{C}$ by replacing the vector $\mathbf{v}_t$ with its nearest code entry $\tilde{\mathbf{v}}_t$ as

$$\tilde{\mathbf{v}}_t = \mathcal{Q}(\mathbf{v}_t), \quad \mathcal{Q}(\mathbf{v}_t) = \mathbf{c}_i \quad \text{where} \quad i = \arg\min_i \|\mathbf{c}_i - \mathbf{v}_t\|_2 \tag{1}$$

Here $\mathcal{Q}$ denotes the quantization process. After the quantization, the decoder $\mathcal{D}$ decodes the approximate vectors $\tilde{\mathbf{v}}_t$ to get the original joint information, as

$$\{\tilde{\mathbf{b}}_t\} = \mathcal{D}\left(\{\tilde{\mathbf{v}}_t\}\right) = \mathcal{D}\left(\mathcal{Q}\left(\mathcal{E}\left(\{\mathbf{b}_t\}\right)\right)\right). \tag{2}$$

Speech Signal Processing. We represent speech signals as low-level onset with amplitude and high-level semantics based on the transcript using BERT [11], following recent works [5, 25]. We leverage an audio and text encoder to process them separately and element-wise concatenate the two types of features to represent the speech signals. We then fuse the speech signal into the gesture representation with several layers of Cross Attention, where the gesture feature functions as the query, and the speech feature serves as both the key and value.

3.2. Spatial-Temporal Gesture Generation

Given an audio signal, we employ a transformer-based model to generate body gestures. Unlike prior approaches [5, 25, 41], which treat the entire body as a holistic representation, our method explicitly models the interactions between different gesture groups. Specifically, we introduce two distinct attention mechanisms within the transformer: **spatial attention** and **temporal attention**, as illustrated in Fig. 3. The model first applies spatial attention to capture inter-region relationships within a single frame, followed by temporal attention to model motion dynamics over time. Below, we describe these mechanisms, their strengths, and their limitations.

Spatial Attention. Spatial attention operates across body regions within a single frame, ensuring structural coherence between different body parts while disregarding temporal dependencies. As illustrated in Fig. 3, we rearrange the input tokens such that all time steps are treated as independent batches, allowing attention to be computed only between different body regions at a given moment. The spatial attention mechanism is formulated as:

$$\mathcal{A}_s = \text{SoftMax}(Q_s \cdot K_s/\sqrt{d} + \mathbf{P})V_s, \tag{3}$$

where $Q_s, K_s, V_s \in \mathbb{R}^{n \times d}$, with n being the number of body regions and d the feature dimensionality. Before applying spatial attention, we incorporate **spatial positional encodings** to capture the relative positions of different body regions. This mechanism ensures consistency across different body parts in a single frame. However, it does not explicitly model how gestures evolve over time, which is crucial for generating natural motion.

Temporal Attention. Temporal attention, in contrast, operates along the time axis, capturing the motion dynamics of each body region independently. To achieve this, we rearrange the input tokens such that all body regions are treated as separate batches, allowing attention to be computed only across different time steps for each region. The temporal attention mechanism is defined as:

$$\mathcal{A}_t = \text{SoftMax}(Q_t \cdot K_t / \sqrt{d} + \mathbf{P}) V_t, \tag{4}$$

where $Q_t, K_t, V_t \in \mathbb{R}^{T \times d}$, with T being the number of time steps. **Temporal positional encodings** are added before applying attention to ensure that the model learns the sequential nature of motion. This mechanism effectively captures gesture continuity and motion patterns across time. However, it does not consider interactions between different body regions at a given time step, which may lead to inconsistencies in complex gestures involving coordinated limb movements.

Gesture Generator. To fully capture spatial-temporal dependencies, we first apply spatial attention to ensure coherence between body regions at each time step, followed by temporal attention to model motion progression. This sequential design enables our model to learn both intra-frame structural relationships and inter-frame motion dynamics.

Finally, we employ two layers of feed-forward networks (FFN) as in the standard Transformer [35] to further refine the attention features in each generator block. This step enhances feature expressiveness, improving the quality and realism of generated gestures.

3.3. Gesture Latent Shortcut Model

Preliminary: Flow-matching and Shortcut Models. Recent flow-matching models [22, 26] tackle generative modeling by learning an ordinary differential equation (ODE) to transform noise into data. The model defines x_t as a linear interpolation between a data point $x_1 \sim \mathcal{D}$ and a noise point $x_0 \sim \mathcal{N}(0, \mathbb{I})$, where:

$$x_t = (1-t)\, x_0 + t\, x_1 \qquad \text{and} \qquad v_t = x_1 - x_0. \tag{5}$$

Given x_0 and x_1, the velocity v_t is fixed. However, for a given x_t, there are multiple plausible pairs (x_0, x_1), leading to a distribution over possible velocities. Thus, v_t becomes

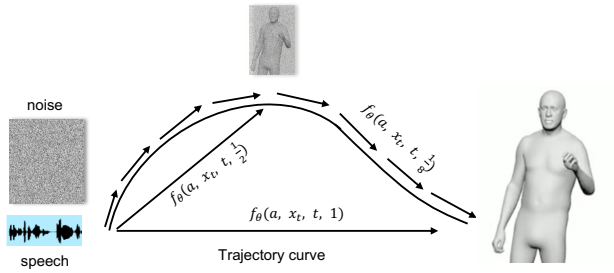

Figure 4. GestureLSM leverages self-consistency along the trajectory during the training conditioned on speech audio.

a random variable. Flow models learn a neural network to estimate the expected velocity: $\bar{v}_t = \mathbb{E}[v_t \mid x_t]$. The model is trained by minimizing the following loss function, which regresses the empirical velocity for randomly sampled pairs (x_0, x_1) from the data distribution:

$$\mathcal{L}^{\text{F}}(\theta) = \mathbb{E}_{x_0, x_1 \sim \mathcal{D}} \left[||\bar{v}_\theta(x_t, t) - (x_1 - x_0)||^2 \right] \tag{6}$$

To sample from the flow model, a noise point x_0 is drawn from a normal distribution and iteratively updated to x_1 via the learned denoising ODE, approximated using Euler sampling.

In contrast, shortcut models [13] address the computational cost of flow-matching by reducing the number of sampling steps. They condition on both the timestep t and a desired step size d, allowing for flexible sampling budgets and faster inference.

Gesture Latent Shortcut. Inspired by the principles of shortcut, we introduce GestureLSM (Latent Shortcut Model), a novel approach to address the challenges of low synthesis efficiency in gesture generation. GestureLSM achieves fast generation speeds while preserving high-quality outputs by leveraging latent shortcut learning on quantized gesture representations. Our model exploits the denoising behavior of shortcut mechanisms, allowing us to devise improved training strategies that enhance overall generation quality and efficiency.

Rather than operating directly in the high-dimensional image pixel space [13], GestureLSM performs learning in a compact, quantized gesture motion space. As depicted in Fig. 4, our model leverages conditioning variable d to model future curvature, enabling the system to anticipate and directly transition to the correct target state.

The normalized direction from the current state x_t to the target state x'_{t+d} is expressed as the shortcut $f_\theta(a, x_t, t, d)$:

$$x'_{t+d} = x_t + f_\theta(a, x_t, t, d). \tag{7}$$

To generalize this process, we train a shortcut model $s_\theta(x_t, t, d)$ that predicts shortcuts for all combinations of

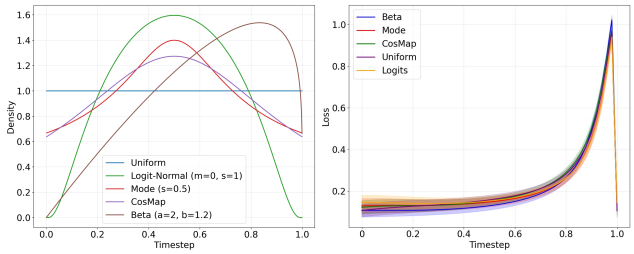

Figure 5. For various time distributions, beta schedule performs the best with left skewed pattern to counteract the ineffectiveness of model prediction when t approaches 1

Table 1. Ablation on the different time distributions, a left skewed pattern will improve the model performance

Distribution.	FGD ↓	BC →	Div. ↑
Uniform	5.051	0.721	13.56
Logit-Normal	4.447	0.755	13.72
Mode	4.532	0.738	13.33
CosMap	4.621	0.742	13.47
α=2 β=1.2	**4.088**	0.714	13.24
α=2 β=1.0	4.123	**0.704**	13.44
α=2.2 β=1.4	4.362	0.754	13.65
α=1.8 β=1.4	4.341	0.743	**13.73**

x_t, t, and d, conditioned on the input speech signal a. To ensure consistency and improve learning, we enforce a self-consistency rule:

$$f_\theta(a, x_t, t, 2d) = \frac{1}{2} f_\theta(a, x_t, t, d) + \frac{1}{2} f_\theta(a, x'_{t+d}, t, d). \tag{8}$$

This rule decomposes the shortcut computation for larger step sizes into a sequence of smaller, intermediate shortcuts. By propagating this capability from multi-step processes to fewer steps and eventually to single steps, the model learns to generate high-quality gestures with minimal computational overhead.

Denoising Pattern Analysis. Prior works have shown that time schedules significantly influence generation quality [12, 19], highlighting the "lost in the middle" problem in flow matching for image generation. These works propose frequent sampling in the middle timesteps to address the issue. However, we observe a distinct pattern in the audio-conditioned gesture generation domain.

As illustrated in Fig. 5, we evaluate various time schedules, including standard uniform sampling [26], Logit-Normal, Heavy-Tails, and CosMap [12]. Across all methods, the loss consistently increases as time steps approach $t \to 1$, indicating poor velocity prediction at the beginning of the trajectory rather than in the middle, as seen in the image domain.

To address this, we hypothesize that a left-skewed sampling distribution can mitigate this issue. We propose using a beta distribution for timestep sampling during training:

$$f(t; \alpha, \beta) = \frac{t^{\alpha-1}(1-t)^{\beta-1}}{\mathrm{B}(\alpha, \beta)}, \quad t \in [0, 1], \tag{9}$$

where α, β controls the skewness of the sampling. The full comparisons of different sampling methods are deferred to the ablation study. From We discover that left skewness with an emphasis when t=1 is important.

4. Experiments

4.1. Datasets

We train and evaluate our models using the BEAT-X dataset proposed by [25]. BEAT-X comprises 60 hours of high-resolution gesture data collected from 25 speakers (12 female, 13 male). The dataset contains 1,762 sequences, each with an average duration of 65.66 seconds, where each sequence captures responses to daily inquiries. For consistency, we adopt the train-validation-test split protocol defined in [25].

4.2. Implementation Details

In the construction of the RVQVAEs, the codebook is initialized uniformly, with each entry having a feature length of 128 and a total size of 1,024 per body region. The codebook updates occur solely during the quantization process, with resets following the Momask strategy [15]. The RVQVAEs are trained for 30,000 iterations, with a learning rate of 2×10^{-4}. The GestureLSM model contains 3 layers of cross-attention for audio-gesture feature fusion and 8 layers of spatial-temporal attention blocks. The latent dimension is set to 256 with feed-forward size of 1024. During the second training stage for speech-to-gesture generation, the codebook remains frozen. We train the GestureLSM model for 1000 epochs. We utilize the Adam optimizer with a learning rate of 2×10^{-4}. All experiments are conducted on a single NVIDIA A100 GPU. We adopt a guidance dropout rate of 0.1 during training and a speech-conditioning ratio of 2 during generation.

4.3. Quantitative Comparisons

Metrics. We evaluate the realism of generated body gestures using the Fréchet Gesture Distance (FGD)[43], which quantifies the distributional similarity between ground truth and synthesized gestures. Diversity[20] is measured by calculating the average L1 distance across multiple gesture clips. To assess speech-motion synchronization, we use Beat Constancy (BC) [21]. For facial motion evaluation,

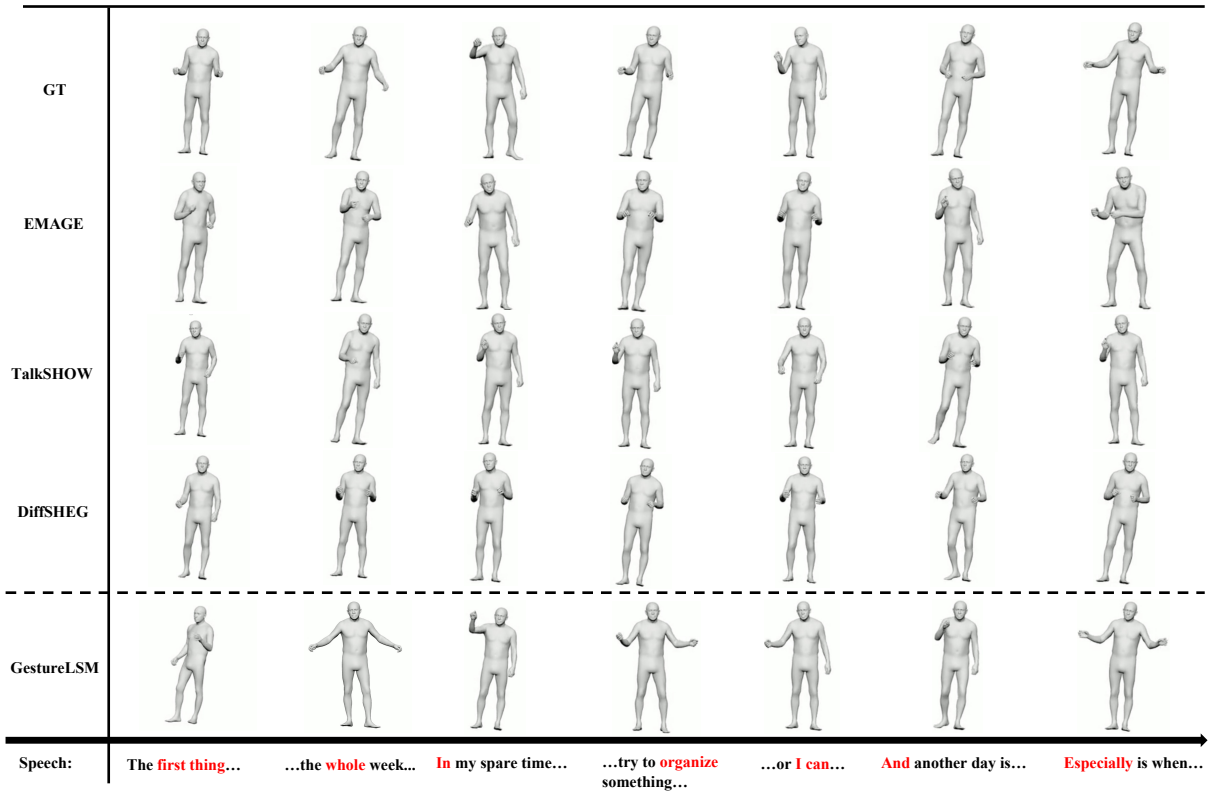

Figure 6. Compared with other methods, GestureLSM presents more natural gesture motions and local body region interactions.

we compute the vertex Mean Squared Error (MSE) [38] to assess positional accuracy. Additionally, the efficiency of our approach is quantified through the Average Inference Time per Sentence (AITS).

Evaluation Results. We summarize the quantitative comparisons with existing methods in Tab. 2. The results highlight that our method achieves state-of-the-art performance across all evaluation metrics. We evaluate two versions of GestureLSM: one focused solely on modeling body gestures and another that integrates both body gestures and facial expressions.

Our method consistently outperforms baseline approaches, achieving a significant reduction in FGD with a score of **4.088**. This improvement stems from our effective modeling of body interactions, which minimizes unnatural gesture patterns during generation. While incorporating facial expressions slightly increases the FGD, the facial expression accuracy remains nearly indistinguishable from the ground truth, as reflected in the substantially lower Mean Squared Error (MSE) for facial expressions.

Moreover, GestureLSM achieves the the most similar BC with the ground-truth, indicating superior synchronization between speech and gestures compared to competing methods. Additionally, our model demonstrates remarkable efficiency, with an average inference speed of **0.039** seconds per frame, significantly surpassing other methods and enabling real-time synthesis.

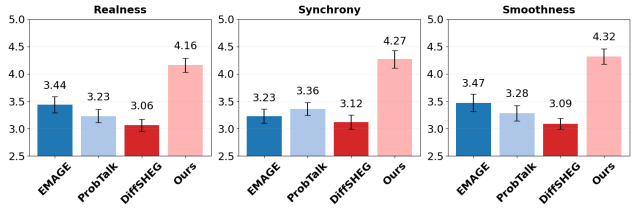

Figure 7. **User Study**. We generate 80 videos per method for evaluations of *Realness*, *Synchrony*, and *Smoothness*.

4.4. Qualitative Comparisons

Evaluation Results As depicted in Figure 6, our approach generates gestures that exhibit improved rhythmic alignment and a more natural appearance compared to existing methods. For example, when conveying the phrase *"the whole week"*, our method directs the subject to extend both hands outward, effectively representing the semantic meaning of *"whole"*. In contrast, competing methods fail to capture this nuance, often generating static or unnatural poses where one or both arms remain down.

Similarly, when interpreting the phrase *"or I can"*, our method raises one hand to emphasize the introduction of an alternative, aligning naturally with conversational cues.

Table 2. Quantitative results on BEAT-X. FGD (Frechet Gesture Distance) multiplied by 10^{-1}, BC (Beat Constancy) multiplied by 10^{-1}, Diversity, MSE (Mean Squared Error) multiplied by 10^{-7}. The best results are in bold.

Methods	Venue	FGD ↓	BC →	Diversity ↑	MSE ↓	AIST ↓
GT			0.703	11.97		
HA2G [27]	CVPR 2022	12.320	0.677	8.626	-	0.195
DisCo [23]	ACMMM 2022	9.417	0.643	9.912	-	0.155
CaMN [24]	ECCV 2022	6.644	0.676	10.86	-	0.675
DiffSHEG [6]	CVPR 2024	7.141	0.743	8.21	9.571	0.066
TalkShow [41]	CVPR 2023	6.209	0.695	13.47	7.791	0.124
ProbTalk [29]	CVPR 2024	5.040	0.771	13.27	8.614	0.151
EMAGE [25]	CVPR 2024	5.512	0.772	13.06	7.680	0.174
MambaTalk [40]	NeurIPS 2024	5.409	0.793	13.07	7.512	-
GestureLSM (w/o face)	-	**4.088**	**0.714**	13.24	-	**0.039**
GestureLSM (holistic)	-	**4.247**	0.729	**13.76**	**1.021**	0.042

Other methods, however, produce awkward gestures, such as raising both hands, which results in unrealistic body interactions. A comparable discrepancy is observed with the phrase *"And another day is"*, where our model captures more contextually appropriate gestures.

For the phrase *"Especially is when"*, our method generates outward hand movements to emphasize the point being made, successfully reflecting the speaker's intent. While minor variations in left and right arm movements may deviate from the ground truth, the overall motion remains semantically consistent and visually coherent.

User Study. We conducted a user study with 20 participants and 320 video samples—80 from each of GestureLSM, EMAGE [25], ProbTalk [29], and DiffSHEG [6]—to evaluate the quality of our results. Each participant viewed the videos in a randomized order and rated them on a scale of 1 (lowest) to 5 (highest) based on three criteria: (1) *realness*, (2) speech-gesture *synchrony*, and (3) *smoothness*.

For **realness**, participants assessed how closely the generated gestures resembled natural human movements in terms of authenticity and fluidity. For **synchrony**, they examined the timing of gestures relative to speech rhythm, audio, and facial expressions to ensure a cohesive performance. For **smoothness**, they analyzed motion continuity, identifying abrupt stops, unnatural jerks, and overall body coordination.

As shown in Fig. 7, GestureLSM outperforms other methods across all criteria, achieving higher Mean Opinion Scores (MOS) and demonstrating improved motion accuracy and better alignment with speech by a large margin.

4.5. Ablation Studies

Gesture Representation. We evaluate gesture quantization methods: (1) w/o quant: Directly use 6D-rotations of joints, (2) one quant: Single VQ quantizer for the whole body. (3) one residual: Single RVQ quantizer for the whole body. (4) product quant: 2D quantizer based on ProbTalk [29]. Tab. 3a shows RVQ outperforms VQ and product quantization. Separating body regions further improves performance over holistic representations.

Model Architecture Design. We analyze architectural variations: (1) attention: Replace spatial-temporal attention with standard attention [35]. (2) w/o spatial: Only temporal attention. (3) w/o temporal: Only spatial attention. (4) w/o position: Remove spatial and temporal positional encodings. Tab. 3b shows spatial temporal attention achieves the best results, with positional encoding providing gains.

Sampling Steps. Performance with different sampling steps is shown in Tab. 3c. Even with 2 steps, the model achieves an FGD of 4.988 with an inference time of 0.018, already outperforming prior methods. Additional steps refine performance further. We take 8 steps for inference efficiency and high generation quality.

Feature Contributions. We assess feature variations: (1) w/o text: Exclude speech transcripts. (2) wavLM: Replace the CNN audio encoder with pretrained WavLM [7]. (3) concatenate: Use concatenation with an MLP for fusion instead of cross-attention. (4) addition: Element-wise addition of speech and gesture features. Tab. 3d shows cross-attention consistently outperforms other fusion methods, while WavLM provides no advantage.

Table 3. Ablations of our method. We exam the gesture representation, model architecture design, number of sampling steps, speech feature processing and model type analysis. Bold indicates the best performance.

Represent.	FGD↓	BC→	Div.↑
w/o quant	8.727	0.612	**13.56**
one quant	6.343	0.734	13.42
one residual	5.256	0.755	13.35
product quant	4.412	0.737	13.41
Ours	**4.088**	**0.714**	13.24

(a) Gesture Motion Representation.

Architecture.	FGD↓	BC→	Div.↑
attention	4.762	0.734	13.43
w/o spatial	8.232	0.766	**14.52**
w/o temporal	22.412	0.454	13.41
w/o position	4.523	0.656	14.23
Ours	**4.088**	**0.714**	13.24

(b) Model Architecture Design.

Steps.	FGD↓	BC→	Div.↑	AIST↓
1	6.235	0.647	13.23	**0.015**
2	4.988	0.680	13.39	0.018
4	4.262	**0.704**	**13.35**	0.026
8	4.088	0.714	**13.24**	0.039
20	**4.040**	0.730	13.49	0.076

(c) Number of sampling steps.

Features.	FGD↓	BC→	Div.↑
w/o text	4.323	0.743	13.17
w WavLM	4.567	**0.707**	13.23
concatenate	4.676	5.479	11.67
addition	6.012	6.234	13.11
cross-atten	**4.088**	0.714	**13.24**

(d) Speech feature processing.

Guidance.	FGD↓	BC→	Div.↑
1.0	4.215	0.741	12.79
1.5	4.141	0.730	13.26
2.0	**4.088**	0.714	13.24
2.5	4.124	0.714	13.61
3.0	4.157	**0.709**	**13.75**

(e) Class Free Guidance.

Model Type.	FGD↓	BC→	Tr-Time↓	AIST↓
Diffusion	4.131	13.06	**1**	2.942
+LCM	4.445	13.17	2.5	0.026
RecFlow	4.724	13.21	**1**	0.074
+ distill	4.761	13.19	2	**0.018**
ours	**4.088**	**13.24**	1.2	0.039

(f) Generation Model Type.

Class Free Guidance. We evaluate guidance scale for conditional generation. We show their performance by the same number of sampling steps of 8. Tab.3e shows a guidance scale of 2 achieves the best performance.

Model Type. To isolate the impact of model type and design, we compare: (1) Diffusion: Use DDPM [16]. (2) +LCM: Following MotionLCM [8], we add latent consistency distillation for the previous setting. (3) ReFlow: Use rectified flow [26]. (4) + distill: Distill the ReFlow model. To validate the training efficiency, we let Diffusion and ReFlow training time as one unit time. Tab. 3f shows Diffusion achieves slight inferior performance with slow inference speed. Latent consistency distillation fails to match our method's training efficiency or performance. ReFlow trains faster but under-performs, even with our proposed optimized time scheduling. our latent shortcut outperforms all these works with only 1.2 unit of training time. Note that further distillations can be also applied to our latent shortcut model, for which we leave to future works.

4.6. Application

In Fig. 8, we show two videos that are generated based on our synthesized gesture motion sequences. As a vital application direction, users can leverage GestureLSM to first generate the 3D-SMPL [31] poses and projected to 2D spaces as gesture keypoints for customized avatar animations with the assistance of off-the-shelf motion-guided video generation technology like AnimateAnyone [17], users can freely create videos for their favorite characters.

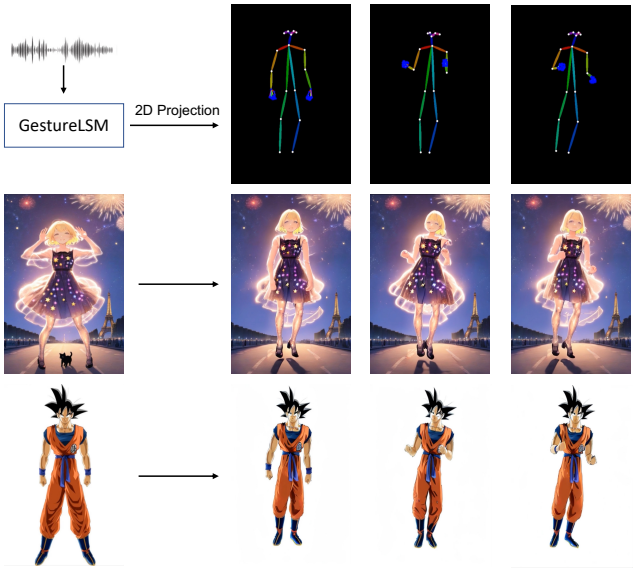

Figure 8. **Avatar Video Generation Application.** After generating a sequence of gesture motions conditioned on speech audio by GestureLSM, we project the 3D keypoints to a 2D plane, serving as keypoint guidance for avatar video generation based on 2D animation methods like AnimateAnyone [17]

5. Conclusion

We present **GestureLSM**, a latent shortcut framework that achieves real time speech driven gesture generation. Our method explicitly represent the gesture into different body regions and leverage spatial and temporal attentions to model their interactions. To leverage shortcut model for the gesture generation framework, we further analyze the denoising patterns of speech-gesture modality and propose an effective time distribution sampling for training. Extensive comparisons with state-of-the-art methods show that **GestureLSM** improves co-speech gesture generation and achieves real time inference for various downstream applications. Future directions may extend our method to fine-grained speech-guided image-to-video generation.

References

[1] Tenglong Ao, Qingzhe Gao, Yuke Lou, Baoquan Chen, and Libin Liu. Rhythmic gesticulator: Rhythm-aware co-speech gesture synthesis with hierarchical neural embeddings. *ACM Transactions on Graphics (TOG)*, 41(6):1–19, 2022. 1

[2] Andreas Blattmann, Tim Dockhorn, Sumith Kulal, Daniel Mendelevitch, Maciej Kilian, Dominik Lorenz, Yam Levi, Zion English, Vikram Voleti, Adam Letts, Varun Jampani, and Robin Rombach. Stable Video Diffusion: Scaling Latent Video Diffusion Models to Large Datasets, 2023. 2

[3] Judee K Burgoon, Thomas Birk, and Michael Pfau. Nonverbal Behaviors, Persuasion, and Credibility. *Human communication research*, 17(1):140–169, 1990. 1

[4] Caroline Chan, Shiry Ginosar, Tinghui Zhou, and Alexei A Efros. Everybody Dance Now. In *ICCV*, 2019. 2

[5] Bohong Chen, Yumeng Li, Yao-Xiang Ding, Tianjia Shao, and Kun Zhou. Enabling synergistic full-body control in prompt-based co-speech motion generation. In *Proceedings of the 32nd ACM International Conference on Multimedia*, page 10, New York, NY, USA, 2024. ACM. 1, 2, 3

[6] Junming Chen, Yunfei Liu, Jianan Wang, Ailing Zeng, Yu Li, and Qifeng Chen. DiffSHEG: A Diffusion-Based Approach for Real-Time Speech-driven Holistic 3D Expression and Gesture Generation, 2024. 2, 7

[7] Sanyuan Chen, Chengyi Wang, Zhengyang Chen, Yu Wu, Shujie Liu, Zhuo Chen, Jinyu Li, Naoyuki Kanda, Takuya Yoshioka, Xiong Xiao, et al. WavLM: Large-Scale Self-Supervised Pre-Training for Full Stack Speech Processing. *IEEE Journal of Selected Topics in Signal Processing*, 16 (6):1505–1518, 2022. 7

[8] Wenxun Dai, Ling-Hao Chen, Jingbo Wang, Jinpeng Liu, Bo Dai, and Yansong Tang. Motionlcm: Real-time controllable motion generation via latent consistency model. *arXiv preprint arXiv:2404.19759*, 2024. 8

[9] Jan P De Ruiter, Adrian Bangerter, and Paula Dings. The Interplay Between Gesture and Speech in the Production of Referring Expressions: Investigating the Tradeoff Hypothesis. *Topics in cognitive science*, 4(2):232–248, 2012. 1

[10] Anna Deichler, Shivam Mehta, Simon Alexanderson, and Jonas Beskow. Diffusion-based co-speech gesture generation using joint text and audio representation. In *INTERNATIONAL CONFERENCE ON MULTIMODAL INTERACTION*. ACM, 2023. 2

[11] Jacob Devlin. BERT: Pre-Training of Deep Bidirectional Transformers for Language Understanding. *arXiv preprint arXiv:1810.04805*, 2018. 3

[12] Patrick Esser, Sumith Kulal, Andreas Blattmann, Rahim Entezari, Jonas Müller, Harry Saini, Yam Levi, Dominik Lorenz, Axel Sauer, Frederic Boesel, Dustin Podell, Tim Dockhorn, Zion English, Kyle Lacey, Alex Goodwin, Yannik Marek, and Robin Rombach. Scaling rectified flow transformers for high-resolution image synthesis, 2024. 5

[13] Kevin Frans, Danijar Hafner, Sergey Levine, and Pieter Abbeel. One step diffusion via shortcut models, 2024. 2, 4

[14] S. Ginosar, A. Bar, G. Kohavi, C. Chan, A. Owens, and J. Malik. Learning Individual Styles of Conversational Gesture. In *CVPR*. IEEE, 2019. 2

[15] Chuan Guo, Yuxuan Mu, Muhammad Gohar Javed, Sen Wang, and Li Cheng. Momask: Generative masked modeling of 3d human motions. In *Proceedings of the IEEE/CVF Conference on Computer Vision and Pattern Recognition*, pages 1900–1910, 2024. 5

[16] Jonathan Ho, Ajay Jain, and Pieter Abbeel. Denoising diffusion probabilistic models, 2020. 2, 8

[17] Li Hu, Xin Gao, Peng Zhang, Ke Sun, Bang Zhang, and Liefeng Bo. Animate Anyone: Consistent and Controllable Image-to-Video Synthesis for Character Animation. *arXiv preprint arXiv:2311.17117*, 2023. 8

[18] Doyup Lee, Chiheon Kim, Saehoon Kim, Minsu Cho, and Wook-Shin Han. Autoregressive Image Generation Using Residual Quantization, 2022. 3

[19] Sangyun Lee, Zinan Lin, and Giulia Fanti. Improving the training of rectified flows, 2024. 5

[20] Jing Li, Di Kang, Wenjie Pei, Xuefei Zhe, Ying Zhang, Zhenyu He, and Linchao Bao. Audio2gestures: Generating diverse gestures from speech audio with conditional variational autoencoders. In *Proceedings of the IEEE/CVF International Conference on Computer Vision*, pages 11293–11302, 2021. 5

[21] Ruilong Li, Shan Yang, David A Ross, and Angjoo Kanazawa. AI Choreographer: Music Conditioned 3D Dance Generation with AIST++. In *Proceedings of the IEEE/CVF International Conference on Computer Vision*, pages 13401–13412, 2021. 5

[22] Yaron Lipman, Ricky TQ Chen, Heli Ben-Hamu, Maximilian Nickel, and Matt Le. Flow Matching for Generative Modeling. *arXiv preprint arXiv:2210.02747*, 2022. 4

[23] Haiyang Liu, Naoya Iwamoto, Zihao Zhu, Zhengqing Li, You Zhou, Elif Bozkurt, and Bo Zheng. DisCo: Disentangled Implicit Content and Rhythm Learning for Diverse Co-Speech Gestures Synthesis. In *Proceedings of the 30th ACM International Conference on Multimedia*, pages 3764–3773, 2022. 1, 7

[24] Haiyang Liu, Zihao Zhu, Naoya Iwamoto, Yichen Peng, Zhengqing Li, You Zhou, Elif Bozkurt, and Bo Zheng. BEAT: A Large-Scale Semantic and Emotional Multi-Modal Dataset for Conversational Gestures Synthesis. *arXiv preprint arXiv:2203.05297*, 2022. 2, 7

[25] Haiyang Liu, Zihao Zhu, Giorgio Becherini, Yichen Peng, Mingyang Su, You Zhou, Naoya Iwamoto, Bo Zheng, and Michael J Black. EMAGE: Towards Unified Holistic Co-Speech Gesture Generation via Masked Audio Gesture Modeling. *arXiv preprint arXiv:2401.00374*, 2023. 1, 2, 3, 5, 7

[26] Xingchao Liu, Chengyue Gong, and Qiang Liu. Flow straight and fast: Learning to generate and transfer data with rectified flow, 2022. 2, 4, 5, 8

[27] Xian Liu, Qianyi Wu, Hang Zhou, Yinghao Xu, Rui Qian, Xinyi Lin, Xiaowei Zhou, Wayne Wu, Bo Dai, and Bolei Zhou. Learning Hierarchical Cross-Modal Association for Co-Speech Gesture Generation. In *CVPR*, pages 10462–10472, 2022. 1, 2, 7

[28] Xingchao Liu, Xiwen Zhang, Jianzhu Ma, Jian Peng, et al. Instaflow: One step is enough for high-quality diffusion-based text-to-image generation. In *The Twelfth International Conference on Learning Representations*, 2023. 2

[29] Yifei Liu, Qiong Cao, Yandong Wen, Huaiguang Jiang, and Changxing Ding. Towards variable and coordinated holistic co-speech motion generation. *arXiv preprint arXiv:2404.00368*, 2024. 7

[30] Simian Luo, Yiqin Tan, Longbo Huang, Jian Li, and Hang Zhao. Latent consistency models: Synthesizing high-resolution images with few-step inference. *arXiv preprint arXiv:2310.04378*, 2023. 2

[31] Georgios Pavlakos, Vasileios Choutas, Nima Ghorbani, Timo Bolkart, Ahmed A. A. Osman, Dimitrios Tzionas, and Michael J. Black. Expressive Body Capture: 3D Hands, Face, and Body from a Single Image. In *CVPR*, 2019. 2, 8

[32] Ludan Ruan, Yiyang Ma, Huan Yang, Huiguo He, Bei Liu, Jianlong Fu, Nicholas Jing Yuan, Qin Jin, and Baining Guo. MM-Diffusion: Learning Multi-Modal Diffusion Models for Joint Audio and Video Generation. In *CVPR*, 2023. 2

[33] Axel Sauer, Frederic Boesel, Tim Dockhorn, Andreas Blattmann, Patrick Esser, and Robin Rombach. Fast high-resolution image synthesis with latent adversarial diffusion distillation. In *SIGGRAPH Asia 2024 Conference Papers*, pages 1–11, 2024. 2

[34] Yang Song, Prafulla Dhariwal, Mark Chen, and Ilya Sutskever. Consistency models. *arXiv preprint arXiv:2303.01469*, 2023. 2

[35] Ashish Vaswani, Noam Shazeer, Niki Parmar, Jakob Uszkoreit, Llion Jones, Aidan N. Gomez, Lukasz Kaiser, and Illia Polosukhin. Attention is all you need, 2023. 4, 7

[36] Fu-Yun Wang, Ling Yang, Zhaoyang Huang, Mengdi Wang, and Hongsheng Li. Rectified diffusion: Straightness is not your need in rectified flow, 2024. 2

[37] Ting-Chun Wang, Ming-Yu Liu, Jun-Yan Zhu, Andrew Tao, Jan Kautz, and Bryan Catanzaro. High-Resolution Image Synthesis and Semantic Manipulation with Conditional GANs. In *CVPR*, 2018. 2

[38] Jinbo Xing, Menghan Xia, Yuechen Zhang, Xiaodong Cun, Jue Wang, and Tien-Tsin Wong. Codetalker: Speech-driven 3d facial animation with discrete motion prior. In *Proceedings of the IEEE/CVF Conference on Computer Vision and Pattern Recognition*, pages 12780–12790, 2023. 6

[39] Zunnan Xu, Yachao Zhang, Sicheng Yang, Ronghui Li, and Xiu Li. Chain of generation: Multi-modal gesture synthesis via cascaded conditional control, 2023. 2

[40] Zunnan Xu, Yukang Lin, Haonan Han, Sicheng Yang, Ronghui Li, Yachao Zhang, and Xiu Li. Mambatalk: Efficient holistic gesture synthesis with selective state space models, 2024. 1, 2, 7

[41] Hongwei Yi, Hualin Liang, Yifei Liu, Qiong Cao, Yandong Wen, Timo Bolkart, Dacheng Tao, and Michael J Black. Generating Holistic 3D Human Motion from Speech. In *CVPR*, 2023. 1, 2, 3, 7

[42] Tianwei Yin, Michaël Gharbi, Richard Zhang, Eli Shechtman, Fredo Durand, William T Freeman, and Taesung Park. One-step diffusion with distribution matching distillation. In *Proceedings of the IEEE/CVF Conference on Computer Vision and Pattern Recognition*, pages 6613–6623, 2024. 2

[43] Youngwoo Yoon, Bok Cha, Joo-Haeng Lee, Minsu Jang, Jaeyeon Lee, Jaehong Kim, and Geehyuk Lee. Speech Gesture Generation from the Trimodal Context of Text, Audio, and Speaker Identity. *ACM TOG*, 39(6), 2020. 5

[44] Zeyi Zhang, Tenglong Ao, Yuyao Zhang, Qingzhe Gao, Chuan Lin, Baoquan Chen, and Libin Liu. Semantic gesticulator: Semantics-aware co-speech gesture synthesis, 2024. 2

[45] Yuanzhi Zhu, Xingchao Liu, and Qiang Liu. Slimflow: Training smaller one-step diffusion models with rectified flow, 2024. 2